Article

Co-Sensitization Strategy with Cascade Energy Level Arrangement for Ultrasensitive Photoelectrochemical Protein Detection

Yan-Hui Zhang, Ying-Ning Zheng, Meng-Jie Li, Tao Hu, Ruo Yuan, and Sha-Ping Wei

Anal. Chem., **Just Accepted Manuscript** • DOI: 10.1021/acs.analchem.8b03740 • Publication Date (Web): 19 Sep 2018

Co-Sensitization Strategy with Cascade Energy Level Arrangement for Ultrasensitive Photoelectrochemical Protein Detection

Yan-Hui Zhang, Ying-Ning Zheng, Meng-Jie Li, Tao Hu, Ruo Yuan*, Sha-Ping Wei*

Key Laboratory of Luminescent and Real-Time Analytical Chemistry (Southwest University), Ministry of Education, College of Chemistry and Chemical Engineering, Southwest University, Chongqing 400715, People's Republic of China

* Corresponding author. Tel.: +86-23-68252277; Fax: +86-23-68253172.

E-mail address: yuanruo@swu.edu.cn (R. Yuan), shapingw@swu.edu.cn (S. P. Wei)

Abstract

Here, a photoelectrochemical (PEC) biosensor was established by a co-sensitization strategy with cascade energy level arrangement for ultrasensitive detection of prostate-specific antigen (PSA). The proposed co-sensitization strategy was based on the well-matched energy level arrangement of four kinds of organic photoactive materials, in which poly{4,8-bis[5-(2-ethylhexyl)thiophen-2-yl]benzo[1,2-b:4,5-b′]dithiophene-2,6-diyl-alt-3-fluoro-2-[(2-ethylhexyl)-carbonyl]thieno[3,4-b]thiophene-4,6-diyl} (PTB7-Th) was used as the photoactive material and perylenetetracarboxyl diimide (PDI), fullerene (nano-C_{60}), polyaniline (PANI) were employed as the sensitizers. The resulted PTB7-Th/PDI/nano-C_{60}/PANI cascade co-sensitization structure with narrow energy level gradient (<0.54 eV) could effectively improve electron transfer capability, obviously raise light energy utilization and significantly enhance photoelectric conversion efficiency, leading to dramatically enhanced photocurrent response. Using PSA as a target model, the proposed PEC biosensor exhibited high sensitivity and excellent stability with a wide detection range from 1 fg/mL to 0.1 ng/mL and a detection limit of 0.43 fg/mL. Moreover, the proposed PEC biosensor provides a cascade co-sensitization strategy that could significantly improve PEC performances and opened up a promising platform to establish high selectivity, stability and ultrasensitive analytical techniques.

Keywords: photoelectrochemical; co-sensitization strategy; cascade energy level arrangement; PTB7-Th

1. Introduction

Photoelectrochemical (PEC) analysis, as a novel and promising analytical technique in the biosensing field, has attracted considerable attention because of its desirable advantages such as simple equipment, low cost, low background signal and high sensitivity.[1-6] Classical PEC sensor commonly requires photoactive material and sensitizer to produce photocurrent response with the addition or generation of electron donor or acceptor.[7-12] However, there are still limitations such as uneven distribution and poor stability of the added electron donor/acceptor. In recent years, a novel donor-acceptor (D-A)-type photoactive material[13, 14] poly{4,8-bis[5-(2-ethylhexyl) thiophen-2-yl]benzo[1,2-b:4,5-b′]dithiophene-2,6-diyl-alt-3-fluoro-2-[(2-ethylhexyl)-carbonyl]thieno[3,4-b]thiophene-4,6-diyl} (PTB7-Th) has gained extensive research interest, which is attributed to the fact that PTB7-Th is different from traditional photoactive materials[15-20] and it can produce continuous photocurrent response without any addition of electron donors or electron acceptors.[21-23] Recently, we constructed two types of PEC sensors by using PTB7-Th as the photoactive material, fullerene (nano-C_{60})[24] and polyaniline (PANI)[25] as the sensitizer, respectively. Although photocurrent response of the above-mentioned works presented great improvements, the deficiencies still existed such as the limited photoelectric conversion efficiency originating from larger energy level gradient between PTB7-Th and its sensitizer. Therefore, it is extremely important to find the energy level arrangement matched photoactive materials with narrow energy level gradient to sensitize PTB7-Th for further improve its photoelectric conversion efficiency.

Perylenetetracarboxyl diimide (PDI) is a n-type semiconductor with good

film-forming ability, excellent stability and high photoelectric conversion efficiency,[26] which has been widely used in organic solar cells as an electron acceptor.[27-29] In particular, the 2.07 eV energy level width of PDI matches well with the 1.58 eV[24] energy level width of PTB7-Th, making PDI an ideal candidate for enhancing the photocurrent signal of PTB7-Th. In view of these inherent advantages of PDI, in this work, we first employed PDI as a sensitizer to enhance the PEC signal of PTB7-Th. In order to further improve the photoelectric conversion efficiency of PTB7-Th, nano-C_{60} (2.60 eV)[24] and PANI (3.0 eV)[30-32] were introduced into this work as sensitizers to form a cascade co-sensitization structure with narrow energy level gradient (<0.54 eV), which could lead to a significantly enhanced photocurrent signal because of its high light energy utilization and strong electron transfer capability.

Herein, a PEC biosensor was proposed by a co-sensitization strategy constructed by four well-matched organic photoactive materials for ultrasensitive detection of prostate-specific antigen (PSA) (Scheme 1). PTB7-Th, PDI, nano-C_{60} were modified on the glassy carbon electrode (GCE) successively, and then gold nanoparticles ($AuNP_S$) were deposited on the modified electrode surface. Subsequently, capture DNA was incubated on the surface of GCE/PTB7-Th/PDI/nano-C_{60}/depAu *via* Au-S bond followed by blocking with hexanethiol (HT). Upon the addition of labeled antibody-DNA1 (DNA1-Ab1), the immunocomplex of capture DNA and DNA1-Ab1 was formed. The introduction of target (PSA) could induce the formation of immunocomplex between detection antibody-DNA2 (DNA2-Ab2) and signal DNA-nano-Au bars, which resulted in proximity-dependent hybridization capture

DNA and signal DNA-nano-Au bars. Under the condition of H_2O_2 and horseradish perxidase (HRP), aniline was polymerized on the signal DNA-nano-Au bars to produce PANI for photocurrent signal amplification. Thereby, the enhanced PEC signal is quantitatively correlated with the concentration of PSA. The successful construction of the as-proposed PEC biosensor based on a co-sensitization strategy can significantly improve the photoelectric conversion efficiency, which paves a new way in early cancer diagnosis, clinical cancer monitoring and various protein detection.

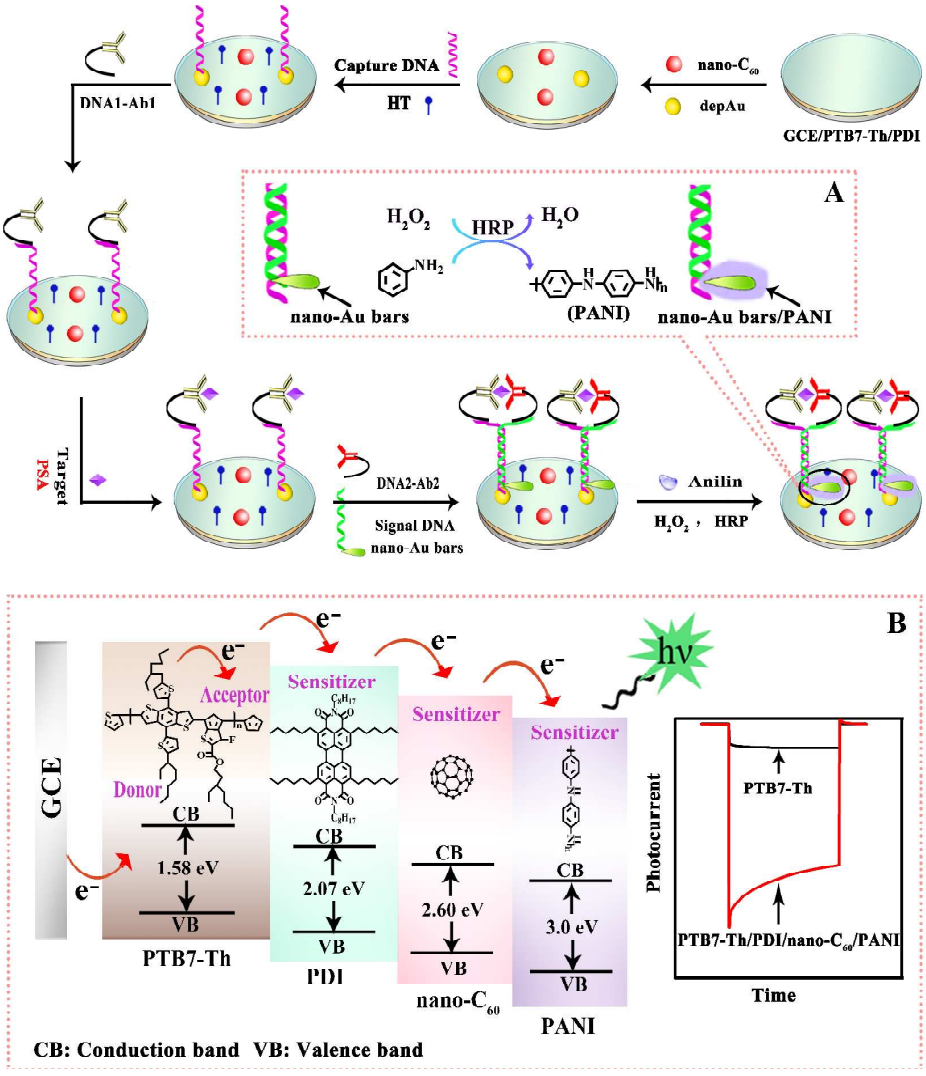

Scheme 1. Schematic illustration of the preparation of PEC biosensor, (A) the situ deposition of PANI on the signal DNA-nano-Au bars under the condition of H_2O_2 and HRP, (B) the electron transfer between four well-matched organic photoactive materials and photocurrent amplification of PTB7-Th by three sensitizers.

2. Experimental Section

2.1 Preparation of Antibody-DNA

Antibody-DNA was accomplished by three steps. First, 0.0002 g hydroxysuccinimide ester (SPDP) was dissolved in 100 μL 95% ethanol to obtain solution A and 0.0015 g dithiothreitol (DTT) was added to 100 μL glacial acetic acid solution to obtain solution B. Second, the 10 μL solution B was added in the 2.5 μM 48 μL DNA1 and 2.5 μM 49 μL DNA2 solution respectively on the shaker react for 1.5 h in 37 ℃ to obtain solution C. At the same time, 100 μL solution A reacted with 100 μL PSA enzyme-labeled antibody for 2 h in 4 ℃ to obtain solution D. Finally, the obtained solution C was mixed with 100 μL solution D respectively to incubate overnight at 4 ℃. The unreacted antibody and DNA were removed and stored at 4 ℃ when not in use.

2.2 Preparation of nano-Au bars

For preparation of the nano-Au bars, briefly, 0.3645 g hexadecyl trimethyi ammonium bromide (CTAB) was dissolved in boiling water and mixed with the 102 μL 1% $HAuCl_4$ to obtain solution A. Then, the mixture of 0.0038 g $NaBH_4$ and 10 mL ice water was added to the solution A and stirred for 10 min to obtain solution B, followed by the stand growth for 3 h. Subsequently, 0.006798 g $AgNO_3$, 1 mM 2.06

mL $HAuCl_4$, 3.645 g CTAB, 0.0176 g ascorbic acid (AA) were mixed with 120 μL solution B. The resulting solution was aged for 20 h to get a uniform solution, which was centrifuged, washed, redispersed in 100 μL phosphate buffer solution (PBS, pH = 7.4, 0.1M) solution and stored at room temperature for use.

2.3 Preparation of Signal DNA-nano-Au bars

For preparation of the signal DNA-nano-Au bars, firstly, 50 μL nano-Au bars solution was dissolved in 500 μL PBS (pH = 7.4, 0.1 M) solution. Then, 50 μL 100 μM signal DNA was mixed with 550 μL nano-Au bars solution though Au-N bond on the shaker for 14 h to obtained signal DNA-nano-Au bars solution, which was centrifuged, washed and stored in -20 ℃ for further use.

2.4 Preparation of PEC Biosensor

The GCE was completely burnished by α-Al_2O_3 powders and then washed ultrasonically in deionized water for several times before modification. Then, the prepared 3 μL PTB7-Th solution was immobilized and filmed on the electrode surface. Afterwards, 7 μL PDI solution and 10 μL nano-C_{60} were attached on the modified PTB7-Th electrode surface successively. Next, the electrodeposition process was accomplished by immersing the electrode in 1% $HAuCl_4$ solution under -0.2 V constant potential for 30 s to deposit $AuNP_S$ (depAu) on the surface of GCE/PTB7-Th/PDI/nano-C_{60}. And the modified electrode was cleaned carefully with deionized water to remove the excess regents, followed by drying in air. Subsequently, 2.5 μM 20 μL capture DNA was incubated on the electrode at room temperature for 14 h to form a self-assembled monolaye[1] (SAM) though Au-S bond. Finally, 1 mM 10

μL HT was added to the modified sensing interface for 45 min to avoid nonspecific adsorption. The unreacted reagents on the electrode were cleaned entirely with deionized water after each step.

2.5 Measurement Procedure

20 μL 2.5 μM DNA1-Ab1 was coated on the modified electrode at 4℃ for 2 h, after that the target (PSA) was dropped on the electrode. Subsequently, 20 μL 2.5 μM DNA2-Ab2 and 20 μL 2.5 μM signal DNA-nano-Au bars were incubated on the obtained electrode for 2 h. Then 10 μL aniline (19 mM, pH = 4.0 adjusted by 0.1 M HI) was dropped on the electrode for 20 min. Next, 0.80 mM HRP and 3.5 mM H_2O_2[33] were immobilized on the electrode to polymerize aniline for 10 min. After the PANI was deposited on the modified electrode, photocurrent can be detected at room temperature. The PEC measurement was performed in 6 mL PBS (pH = 7.0, 0.1 M).

3. Results and Discussion

3.1 Morphology of the Nanomaterials

The morphologies of the PTB7-Th, nano-C_{60}, nano-Au bars and PANI@nano-Au bars were characterized by scanning electron microscopy (SEM). Figure 1A showed the PTB7-Th photograph, which exhibits a wrinkled film structure. The nano-C_{60} showed globular structures at approximate 100 nm (Figure 1B). The SEM photograph of nano-Au bars with needle structure of 1 μM diameter was demonstrated in Figure 1C, indicating the successful synthesis of nano-Au bars. The morphology of the PANI@nano-Au bars showed nanocapsule structures of around 2 μM diameter in Figure 1D, indicating the successful synthesis of PANI@nano-Au bars.

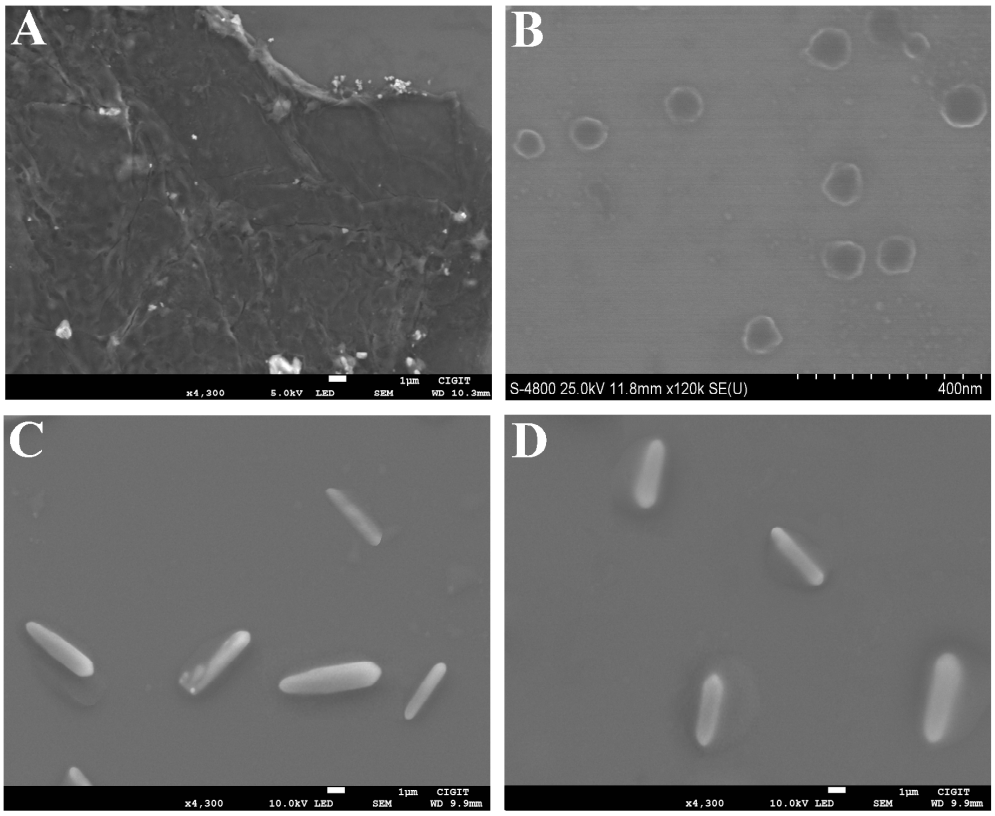

Figure 1. The SEM photographs of PTB7-Th (A), nano-C_{60} (B), nano-Au bars (C) and PANI@nano-Au bars (D).

3.2 Characterization of PEC Biosensor

In order to verify the successful preparation of PEC biosensor, the photocurrent characterizations of each step are shown in Figure 2. PTB7-Th, PDI, nano-C_{60} were drop-cast onto a bare GCE surface successively, the photocurrent intensity increased gradually (curve b, c, d), demonstrating that PTB7-Th, PDI, nano-C_{60} are well-matched photoactive materials for the construction of the PEC biosensor. After AuNPs were deposited, the photocurrent was significantly enhanced (curve e). Then the modifed electrode was incubated with capture DNA, the photocurrent decreased derived from the poor charge transfer of DNA sequence (curve f). As anticipated, a

decreased photocurrent (curve g) was observed after blocking with HT. Subsequently, the photocurrent intensity decreased after immobilization of DNA1-Ab1, PSA (0.1 ng/mL) DNA2-Ab2 and signal DNA-nano-Au bars (curve h). This could be explained by the fact that the immobilization of these macromolecules on the modified electrode hinder the charge transfer. The strongest photocurrent was obtained after in situ deposition of PANI (curve i). The above results show that the PEC biosensor was successfully constructed. To further demonstrate the successful preparation of PEC biosensor, the assembly steps of the sensing interface were characterized by cyclic voltammetry (CV) measurement (Figure S2, Supporting Information).

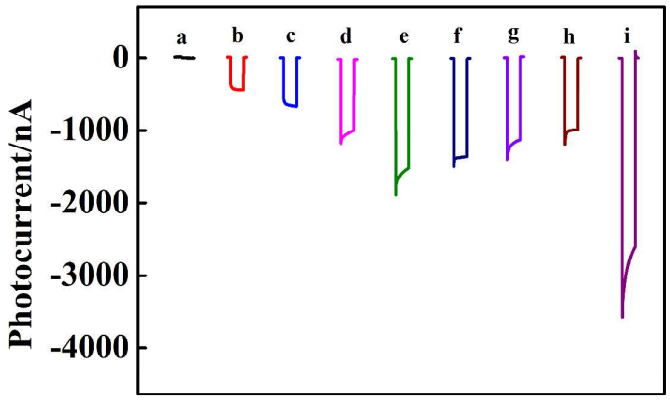

Figure 2. Photocurrent responses of (a) bare GCE, (b) GCE/PTB7-Th, (c) GCE/PTB7-Th/PDI, (d) GCE/PTB7-Th/PDI/nano-C_{60}, (e) GCE/PTB7-Th/PDI/nano-C_{60}/depAu, (f) GCE/PTB7-Th/PDI/nano-C_{60}/depAu/capture DNA, (g) GCE/PTB7-Th/PDI/nano-C_{60}/depAu/capture DNA/HT, (h) GCE/PTB7-Th/PDI/nano-C_{60}/depAu/capture DNA/HT/DNA1-Ab1/PSA/DNA2-Ab2/signal DNA-nano-Au bars and (i) GCE/PTB7-Th/PDI/nano-C_{60}/depAu/capture DNA/HT/DNA1-Ab1/PSA/DNA2-Ab2/signal DNA-nano-Au bars/PANI. The PEC measurement was performed in 6 mL PBS (pH = 7.0, 0.1 M).

3.3 Comparison of PEC Responses for Different Photoactive Materials

For demonstrating the superiority of PDI, nano-C_{60} and PANI as sensitizers for PTB7-Th in this co-sensitization strategy, comparison study was executed by immobilizing different materials on the GCE surface including (A) GCE/PTB7-Th, (B) GCE/PTB7-Th/PDI, (C) GCE/PTB7-Th/PDI/nano-C_{60}, (D) GCE/PTB7-Th/PDI/nano-C_{60}/PANI (aniline was polymerized on the signal DNA-nano-Au bars). The photocurrent responses for different materials were shown in Figure 3. As shown in Figure 3A, when PTB7-Th was modified on bare electrode, about 444 nA photocurrent was observed. In Figure 3B, about 657 nA photocurrent was obtained when PDI was dropped onto the electrode. Then nano-C_{60} was dropped onto the GCE/PTB7-Th/PDI, an increased photocurrent (1047 nA) was observed in Figure 3C. When aniline was polymerized on the signal DNA-nano-Au bars (target PSA, 0.1 ng/mL), a significantly increased photocurrent (2828 nA) was observed in Figure 3D, which was up to 7 times greater than that of PTB7-Th. The results explicitly demonstrated that the sensitizers (PDI, nano-C_{60} and PANI) could significantly improve the photoelectric conversion efficiency of PTB7-Th, leading to a signal amplification. To investigate the enhancement effect of nano-C_{60} and PANI toward PTB7-Th, the PEC responses of different photoactive materials were recorded (Figure S3, Supporting Information).

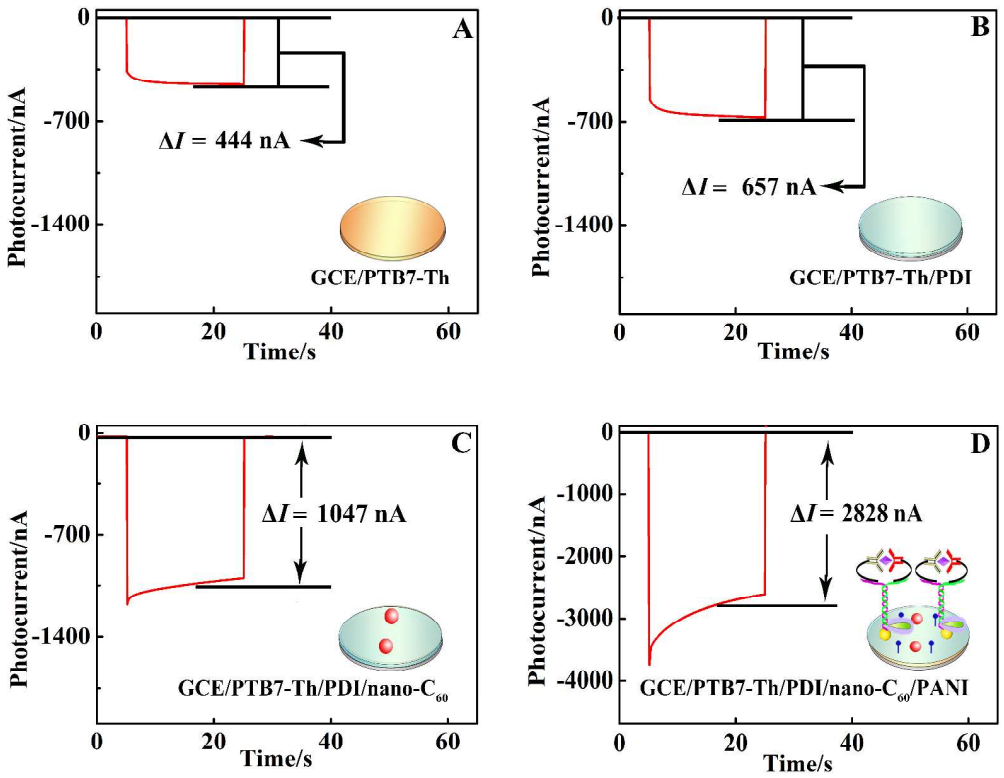

Figure 3. Photocurrent responses of different materials: (A) GCE/PTB7-Th, (B) GCE/PTB7-Th/PDI, (C) GCE/PTB7-Th/PDI/nano-C_{60} and (D) GCE/PTB7-Th/PDI/nano-C_{60}/ PANI (aniline was polymerized on the signal DNA-nano-Au bars).

3.4 Analytical Performance

The excellent performance of the fabricated PEC biosensor was analyzed under optimal experimental conditions (Figure S1, Supporting Information). The photocurrent enhanced as the increased of target PSA concentration (Figure 4A). The linear relationship between the photocurrent and logarithm of PSA concentration showed a wide detection range of 1 fg/mL - 0.1 ng/mL with a detection limit of 0.43 fg/mL (calculated from the expression of 3σ/S, where σ and S stand for the standard deviation of blank and the slope of the calibration curve, respectively) and a linear regression equation of I = - 3035.0 - 213.9 lg$c$ (Figure 4B), with a correlation

coefficient of 0.9953 (where *I* and *c* were the photocurrent and PSA concentration correspondingly). The comparison of previously reported methods for protein detection was shown in Table 1, which exhibited that the fabricated PEC biosensor possessed prominent potential for ultrasensitive detection of PSA.

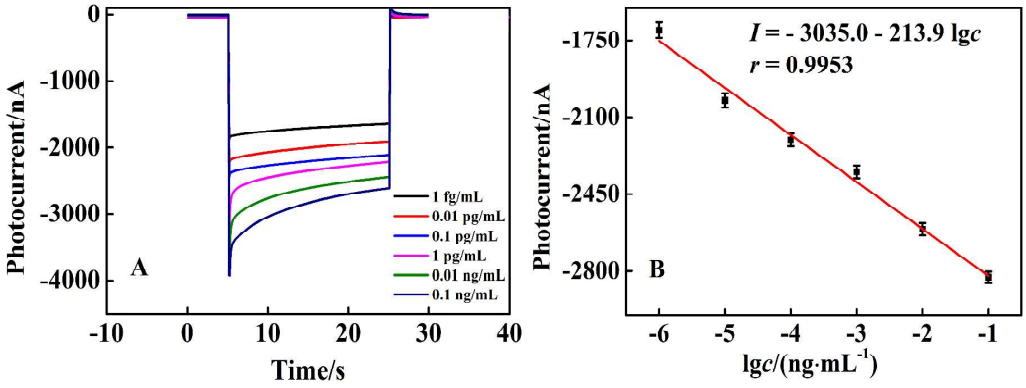

Figure 4. (A) Photocurrent response of the PEC biosensor incubated with PSA of different concentrations, (B) The calibration curve between photocurrent and the logarithm of PSA concentration.

Table 1. Comparison of previously reported methods for protein detection.

detection technology	detection range	detection limit	reference
electrochemical	74 pg/mL - 740 ng/mL	28 pg/mL	34
electrochemical	0.1 pg/mL - 300 pg/mL	30 fg/mL	35
fluorescent	0.05 ng/mL - 20 ng/mL	6.7 pg/mL	36
surface enhanced raman scattering	1 pg/mL - 1000 ng/mL	0.11 pg/mL	37
electrochemiluminescence	1 pg/mL - 10 ng/mL	1 pg/mL	38
electrochemiluminescence	0.0001 ng/mL - 1.0 ng/mL	0.056 pg/mL	39
electrochemiluminescence	0.0001 ng/mL - 50 ng/mL	0.056 pg/mL	40
photoelectrochemical	10 pg/mL - 80 ng/mL	3.0 pg/mL	41
photoelectrochemical	0.01 pg/mL - 50 ng/mL	1.5 pg/mL	42
photoelectrochemical	1.0 fg/mL - 0.1 ng/mL	0.43 fg/mL	our work

3.5 Selectivity and Stability of the PEC Biosensor

To monitor the selectivity of the PEC biosensor, a contrast experiment was studied by incubated different interferences including 0.1 pg/mL CEA, 0.1 pg/mL AFP, 0.1 pg/mL AA, 0.1 pg/mL TB and 0.1 pg/mL Mg^{2+}. The blank experiment was performed by the same method and procedure for constructing PEC biosensor, in which an equal amount of PBS (pH = 7.0) was substituted for the target PSA and the obtained photocurrent signal was used as the blank value. As shown in Figure 5A, there was no apparent photocurrent response for the interferences compared with target PSA (1 fg/mL), which indicated the constructed PEC biosensor possessed good selectivity. Figure 5B exhibited the stability of the as-prepared PEC biosensor incubated with 0.1 pg/mL PSA under successive periodic off-on light irradiation for 10 cycles with LED lamp excitation. The relative standard deviation (RSD) was 3.17%, which demonstrated an expected stability of the fabricated PEC biosensor for ultrasensitive detection of PSA.

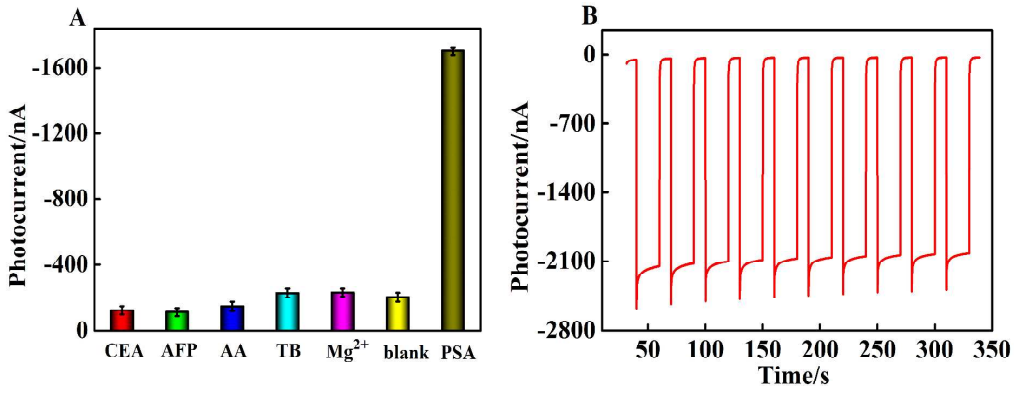

Figure 5. (A) Selectivity of PEC biosensor toward common interferences: CEA, AFP, AA, TB, Mg^{2+} and the blank, (B) Stability of PEC biosensor incubated with 0.1 pg/mL PSA.

3.6 Analysis of Clinical Serum Samples

In order to assess the potential application of our PEC biosensor, clinical serum samples of various patients (obtained from the Xinqiao Hospital of Chongqing, China) were further analyzed. The results of the assay were compared with reference values for commercial PSA ELISA kit. As shown in Table 2, no significant differences between the two methods were obtained in the analysis of six samples, which indicated that the proposed method had potential application for the detection of clinical samples. Furthermore, the detailed content of recovery tests was added in Table S2 (Supporting Information).

Table 2. Assay results of clinical serum samples using the proposed method and PSA ELISA kit.

Sera sample	Add concentration/pg mL^{-1}	mean/pg mL^{-1} ± SD, n=3		Relative error/ %
		Proposed method	PSA ELISA kit	
1	1.0	1.05 ± 1.13	1.04 ± 1.25	0.95
2	5.0	5.27 ± 2.94	5.13 ± 2.62	2.38
3	10	11.32 ± 3.26	10.87 ± 3.02	1.31
4	50	50.23 ± 3.64	49.72 ± 2.71	2.07
5	100	99.34 ± 2.57	100.52 ± 3.12	-3.34
6	500	501.73 ± 4.08	500.31 ± 3.23	1.57

4. Conclusion

In summary, an ultrasensitive PEC biosensor was constructed based on a co-sensitization strategy with use of PTB7-Th as the photoactive material and PDI, nano-C_{60}, PANI as the sensitizers. The obtained PTB7-Th/PDI/nano-C_{60}/PANI co-sensitization structure possessed a cascade energy level arrangement with narrow

energy level gradient (<0.54 eV), which could effectively improve photoelectric conversion efficiency, resulting in significantly enhanced photocurrent signal. By employing this cascade co-sensitization strategy, our proposed PEC biosensor exhibited high sensitivity and wide linear range. More importantly, the established PEC strategy has great prospects of application in clinical cancer diagnosis, biological research and other related sciences.

Acknowledgments

This work was financially supported by the National Natural Science Foundation NNSF of China (Grants 21575116, 21675129 and 21775124) and the Fundamental Research Funds for the Central Universities (Grants XDJK2018AA003), China.

Supporting Information

Materials, reagents, apparatus, optimization of experimental conditions, CV characterization of PEC biosensor, comparison of PEC responses for different photoactive materials, analysis of clinical serum samples.

References

(1) Wen, G. M.; Ju, H. X. Enhanced Photoelectrochemical Proximity Assay for Highly Selective Protein Detection in Biological Matrixes. *Anal. Chem.* **2016**, *88*, 8339-8345.

(2) Li, L.; Zhang, Y.; Zhang, L. N.; Ge, S. G.; Liu, H. Y.; Ren, N.; Yan, M.; Yu, J. H. Paper-Based Device for Colorimetric and Photoelectrochemical Quantification of the Flux of H_2O_2 Releasing from MCF-7 Cancer Cells. *Anal. Chem.* **2016**, *88*, 5369-5377.

(3) Zhao, W. W.; Xu, J. J.; Chen, H. Y. Photoelectrochemical Bioanalysis: the State of the Art. *Chem. Soc. Rev.* **2015**, *44*, 729-741.

(4) Jiang, D.; Du, X. J.; Zhou, L.; Li, H. N.; Wang, K. New Insights toward Efficient Charge-Separation Mechanism for High-Performance Photoelectrochemical Aptasensing: Enhanced Charge-Carrier Lifetime via Coupling Ultrathin MoS_2 Nanoplates with Nitrogen-Doped Graphene Quantum Dots. *Anal. Chem.* **2017**, *89*, 4525-4531.

(5) Hao, N.; Zhang, Y.; Zhong, H.; Zhou, Z.; Hua, R.; Qian, J.; Liu, Q.; Li, H.; Wang, K. Design of a Dual Channel Self-Reference Photoelectrochemical Biosensor. *Anal. Chem.* **2017**, *89*, 10133-10136.

(6) Zhang, N.; Ruan, Y. F.; Zhang, L. B.; Zhao, W. W.; Xu, J. J.; Chen, H. Y. Nanochannels Photoelectrochemical Biosensor. *Anal. Chem.* **2018**, *90*, 2341-2347.

(7) Chang, Y. S.; Choi, M.; Beak, M.; Hsieh, P. Y.; Yong, K.; Hsu, Y. J. CdS/CdSe Co-Sensitized Brookite H:TiO_2 Nanostructures: Charge Carrier Dynamics and Photoelectrochemical Hydrogen Generation. *Appl. Catal., B* **2018**, *225*, 379-385.

(8) Ruan, Y. F.; Zhang, N.; Zhu, Y. C.; Zhao, W. W.; Xu, J. J.; Chen, H. Y. Photoelectrochemical Bioanalysis Platform of Gold Nanoparticles Equipped Perovskite Bi_4NbO_8Cl. *Anal. Chem.* **2017**, *89*, 7869-7875.

(9) Pareek, A.; Kim, H. G.; Paik, P.; Borse, P. H. Ultrathin MoS_2-MoO_3 Nanosheets Functionalized CdS Photoanodes for Effective Charge Transfer in Photoelectrochemical (PEC) Cells. *J. Mater. Chem. A* **2017**, *5*, 1541-1547.

(10) Li, H. B.; Li, J.; Zhu, Y. Y.; Xie, W. Y.; Shao, R.; Yao, X. X.; Gao, A. Q.; Yin, Y. D. Cd^{2+}-Doped Amorphous TiO_2 Hollow Spheres for Robust and Ultrasensitive Photoelectrochemical Sensing of Hydrogen Sulfide. *Anal. Chem.* **2018**, *90*, 5496-5502.

(11) Sun, B.; Dong, J.; Shi, W. J.; Ai, S. Y. A Hierarchical Charge Transport Cascade Based on

W-Bi_2S_3/poly(thiophenyl-3-boronic acid) Hybrid for Robust Photoelectrochemical Analysis of Subgroup J of Avian Leukosis Virus. *Sensors and Actuators B*. **2016**, *229*, 75-81.

(12) Li, X.; Zhu, L. S.; Zhou, Y. L.; Yin, H. S.; Ai, S. Y. Enhanced Photoelectrochemical Method for Sensitive Detection of Protein Kinase A Activity Using TiO_2/g-C_3N_4, PAMAM Dendrimer, and Alkaline Phosphatase. *Anal. Chem*. **2017**, *89*, 2369-2376.

(13) Liao, S. H.; Jhuo, H. J.; Cheng, Y. S.; Chen, S. A. Fullerene Derivative□Doped Zinc Oxide Nanofilm as the Cathode of Inverted Polymer Solar Cells with Low□Bandgap Polymer (PTB7□Th) for High Performance. *Adv. Mater.* **2013**, *25*, 4766-4771.

(14) Sukegawa, J.; Schubert, C.; Zhu, X. Z.; Tsuji, H.; Guldi, D. M.; Nakamura, E. Electron Transfer Through Rigid Organic Molecular Wires Enhanced by Electronic and Electron-Vibration Coupling. *Nat. Chem*. **2014**, *6*, 899-905.

(15) Li, Y. J.; Ma, M. J.; Zhu, J. J. Dual-Signal Amplification Strategy for Ultrasensitive Photoelectrochemical Immunosensing of α-Fetoprotein. *Anal. Chem.* **2012**, *84*, 10492-10499.

(16) Shen, Q. M.; Han, L.; Fan, G. C.; Zhang, J. R.; Jiang, L. P.; Zhu, J. J. "Signal-On" Photoelectrochemical Biosensor for Sensitive Detection of Human T-Cell Lymphotropic Virus Type II DNA: Dual Signal Amplification Strategy Integrating Enzymatic Amplification with Terminal Deoxynucleotidyl Transferase-Mediated Extension. *Anal. Chem*. **2015**, *87*, 4949-4956.

(17) Zhu, Y. C.; Zhang, N.; Ruan, Y. F.; Zhao, W. W.; Xu, J. J.; Chen, H. Y. Alkaline Phosphatase Tagged Antibodies on Gold Nanoparticles/TiO_2 Nanotubes Electrode: A Plasmonic Strategy for Label-Free and Amplified Photoelectrochemical Immunoassay. *Anal. Chem*. **2016**, *88*, 5626-5630.

(18) Fan, G. C.; Shi, X. M.; Zhang, J. R.; Zhu, J. J. Cathode Photoelectrochemical Immunosensing Platform Integrating Photocathode with Photoanode. *Anal. Chem*. **2016**, *88*, 10352 10356.

(19) Zhao, W. W.; Ma, Z. Y.; Yan, D. Y.; Xu, J. J.; Chen, H. Y. In Situ Enzymatic Ascorbic Acid Production as Electron Donor for CdS Quantum Dots Equipped TiO_2 Nanotubes: A General and Efficient Approach for New Photoelectrochemical Immunoassay. *Anal. Chem.* **2012**, *84*, 10518-10521.

(20) Zhao, W. W.; Ma, Z. Y.; Yu, P. P.; Dong, X. Y.; Xu, J. J; Chen, H. Y. Highly Sensitive Photoelectrochemical Immunoassay with Enhanced Amplification Using Horseradish Peroxidase Induced Biocatalytic Precipitation on a CdS Quantum Dots Multilayer Electrode. Y. *Anal. Chem.* **2012**, *84*, 917-923.

(21) Beaujuge, P. M.; Pisula, W.; Tsao, H. N.; Ellinger, S.; Müllen, K.; Reynolds, J. R. Tailoring Structure-Property Relationships in Dithienosilole-Benzothiadiazole Donor-Acceptor Copolymers. *J. Am. Chem. Soc.* **2009**, *131*, 7514-7515.

(22) Blouin, N.; Michaud, A.; Leclerc, M. A Low-Bandgap Poly(2,7-Carbazole) Derivative for Use in High‐Performance Solar Cells. *Adv. Mater.* **2007**, *19*, 2295-2300.

(23) Cho, S.; Seo, J. H.; Kim, G. H.; Kim, J. Y.; Woo, H. Y. J. Observation of Ambipolar Field-Effect Behavior in Donor–Acceptor Conjugated Copolymers. *Mater. Chem.* **2012**, *22*, 21238-21241.

(24) Zheng, Y. N.; Liang, W. B.; Xiong, C. Y.; Yuan, Y. L.; Chai, Y. Q.; Yuan, R. Self-Enhanced Ultrasensitive Photoelectrochemical Biosensor Based on Nanocapsule Packaging Both Donor‐Acceptor-Type Photoactive Material and Its Sensitizer. *Anal. Chem.* **2016**, *88*, 8698–8705.

(25) Hu, T.; Zheng, Y. N.; Li, M. J.; Liang, W. B.; Chai, Y. Q.; Yuan, R. A Highly Sensitive Photoelectrochemical Assay with Donor-Acceptor-Type Material as Photoactive Material and Polyaniline as Signal Enhancer. *Anal. Chem.* **2018**, *90*, 6096-6101.

(26) Hartnett, P. E.; Timalsina, A.; Matte, H. R.; Zhou, N.; Guo, X.; Zhao, W.; Facchetti, A.; Chang, R. P. H.; Hersam, M. C.; Wasielewsk, M. R.; Marks, T. J. Slip-Stacked Perylenediimides as an Alternative Strategy for High Efficiency Nonfullerene Acceptors in Organic Photovoltaics. *J. Am. Chem. Soc.* **2014**, *136(46)*: 16345-16356.

(27) Zhang, J. Q.; Li, Y. K.; Huang, J. C.; Hu, H. W.; Zhang, G. Y.; Ma, T. X.; Chow, P. C. Y.; Ade, H.; Pan, D.; Yan, H. Ring-Fusion of Perylene Diimide Acceptor Enabling Efficient Nonfullerene Organic Solar Cells with a Small Voltage Loss. *J. Am. Chem. Soc.* **2017**, *139*, 16092-16095.

(28) Hwang, Y. J.; Earmme, T.; Courtright, B. A. E.; Eberle, F. N.; Jenekhe, S. A. n-Type Semiconducting Naphthalene Diimide-Perylene Diimide Copolymers: Controlling Crystallinity, Blend Morphology, and Compatibility Toward High-Performance All-Polymer Solar Cells. *J. Am. Chem. Soc.* **2015**, *137*, 4424-4434.

(29) Wu, Z. H.; Sun, C.; Dong, S.; Jiang, X. F.; Wu, S. P.; Wu, H. B.; Yip, H. L.; Huang, F.; Cao, Y. n-Type Water/Alcohol-Soluble Naphthalene Diimide-Based Conjugated Polymers for High-Performance Polymer Solar Cells. *J. Am. Chem. Soc.* **2016**, *138*, 2004-2013.

(30) Catedral, M. D.; Tapia, A. K. G.; Sarmago, R. V. Effect of Dopant Ions on the Electrical Conductivity and Microstructure of Polyaniline (Emeraldine Salt). *Science Diliman* **2007**, *16(2)*, 41-46.

(31) AbdulAlmohsin, S.; Al-Mutoki, S. M.; Li, Z. Fabrication and Characterization of Aluminum-doped ZnO/PANI Hybrid Solar Cells. *Journal of the Arkansas Academy of Science* **2012**, *66(1)*, 26-30.

(32) Hatchett, D. W.; Josowicz, M.; Janata, J. Acid Doping of Polyaniline: Spectroscopic and Electrochemical Studies. *J. Phys. Chem. B* **1999**, *103*, 10992-10998.

(33) Ma, Y. F.; Zhang, J. M.; Zhang, G. J.; He, H. X. Polyaniline Nanowires on Si Surfaces Fabricated with DNA Templates. *J. Am. Chem. Soc.* **2004**, *126(22)*, 7097-7101.

(34) Zhu, J.; Gan,.H Y.; Wu, J.; Ju, H. X. Molecular Machine Powered Surface Programmatic Chain Reaction for Highly Sensitive Electrochemical Detection of Protein. *Anal. Chem.* **2018**, *90*, 5503-5508.

(35) Ren, X.; Ma, H. M.; Zhang, T.; Zhang, Y.; Yan, T.; Du, B.; Wei, Q. Sulfur-Doped Graphene-Based Immunological Biosensing Platform for Multianalysis of Cancer Biomarkers. *ACS Appl. Mater. Interfaces* **2017**, *9*, 37637-37644.

(36) Qiu, Z. L.; Shu, J. and Tang, D. P. Bioresponsive Release System for Visual Fluorescence Detection of Carcinoembryonic Antigen from Mesoporous Silica Nanocontainers Mediated Optical Color on Quantum Dot-Enzyme-Impregnated Paper. *Anal. Chem.* **2017**, *89*, 5152-5160.

(37) Cheng, Z. Y.; Choi, N.; Wang, R.; Lee, S.; Moon, K. C.; Yoon, S. Y.; Chen, L. X.; Choo, J. Simultaneous Detection of Dual Prostate Specific Antigens Using Surface-Enhanced Raman Scattering-Based Immunoassay for Accurate Diagnosis of Prostate Cancer. *ACS Nano* **2017**, *11*, 4926-4933.

(38) Zou, G. Z.; Tan, X.; Long, X. Y.; He, Y. P.; Miao, W. J. Spectrum-Resolved Dual-Color Electrochemiluminescence Immunoassay for Simultaneous Detection of Two Targets with Nanocrystals as Tags. *Anal. Chem.* **2017**, *89*, 13024-13029.

(39) Ma, H. M.; Zhao, Y. H.; Liu, Y. Y.; Zhang, Y.; Wu, D.; Li, H.; Wei, Q. A Compatible Sensitivity Enhancement Strategy for Electrochemiluminescence Immunosensors Based on the Biomimetic Melanin-Like Deposition. *Anal. Chem.* **2017**, *89*, 13049-13053.

(40) Yang, L.; Li, Y. Y.; Zhang, Y.; Fan, D. W.; Pang, X. H.; Wei, Q.; Du, B. 3D Nanostructured

Palladium-Functionalized Graphene-Aerogel┐ Supported Fe_3O_4 for Enhanced $Ru(bpy)_3^{2+}$-Based Electrochemiluminescent Immunosensing of Prostate Specific Antigen. *ACS Appl. Mater. Interfaces* **2017**, *9*, 35260-35267.

(41) Shu, J.; Qiu, Z. L.; Zhou, Q.; Lin, Y. X..; Lu, M. H.; Tang, D. P. Enzymatic Oxydate-Triggered Self-Illuminated Photoelectrochemical Sensing Platform for Portable Immunoassay Using Digital Multimeter. *Anal. Chem.* **2016**, *88*, 2958-2966.

(42) Lv, S.; Zhang, K. Y.; Zeng, Y. Y.; Tang, D. P. Double Photosystems-Based 'Z-Scheme' Photoelectrochemical Sensing Mode for Ultrasensitive Detection of Disease Biomarker Accompanying Three-Dimensional DNA Walker. *Anal. Chem.* **2018**, *90*, 7086-7093.

For TOC only

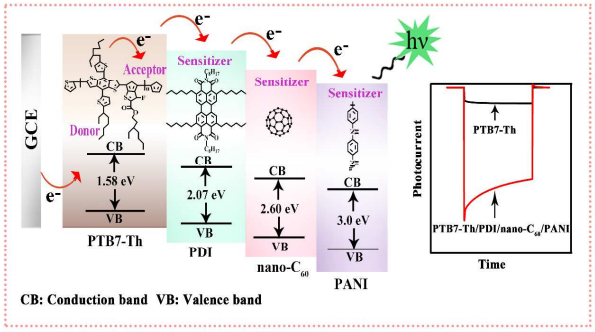
GCE
e⁻
Acceptor
Donor
CB
1.58 eV
VB
PTB7-Th
Sensitizer
CB
2.07 eV
VB
PDI
Sensitizer
CB
2.60 eV
VB
nano-C60
Sensitizer
CB
3.0 eV
VB
PANI
hv
Photocurrent
PTB7-Th
PTB7-Th/PDI/nano-C60/PANI
Time
CB: Conduction band VB: Valence band